

Corsika+Herwig Monte Carlo Simulation of Neutrino Induced Atmospheric Air Showers

M. Ambrosio¹, C. Aramo¹, A. Della Selva¹, G. Miele¹, S. Pastor², O. Pisanti¹,
and L. Rosa¹

¹ *Dipartimento di Scienze Fisiche, Università di Napoli “Federico II” and
Istituto Nazionale di Fisica Nucleare, Sezione di Napoli
Complesso Universitario di Monte S. Angelo, Via Cinthia, I-80126 Napoli, Italy*

² *Instituto de Física Corpuscular (CSIC-Universitat de València),
Edificio Institutos de Investigación, Apdo. 22085, E-46071 Valencia, Spain*

E-mails:

ambrosio@na.infn.it
aramo@na.infn.it
dellaselva@na.infn.it
miele@na.infn.it
pastor@ific.uv.es
pisanti@na.infn.it
rosa@na.infn.it

Abstract

High-energy neutrino astronomy represents an open window both on astrophysical mechanisms of particle acceleration and on fundamental interactions. The possibility of detecting them in large earth-based apparatus, like AUGER, AMANDA, ANTARES, is quite challenging. In view of this, the capability of generating reliable simulations of air showers induced by neutrinos is mandatory in the analysis of experimental data. In this paper we describe preliminary results towards the development of a new version of the Monte Carlo CORSIKA, capable of handling neutrinos too as primary particles. In our approach the first interaction of the primary neutrino is simulated in CORSIKA with a call to the HERWIG event generator.

1 Introduction

A large variety of astrophysical and exotic sources are expected to emit ultra-high energy (UHE) particles and among them also neutrinos. The observation of Extensive Air Showers (EAS) [1] with energy larger than 10^{20} eV implies in any theoretical scenario the simultaneous presence of a flux of UHE ν 's. This is particularly clear reminding that such energetic events are either originated in an astrophysical source (bottom-up models) or are the consequence of the decay of massive Big Bang relic particles (top-down scenarios) [2]. The bottom-up acceleration mechanisms occur in astrophysical environments, such as Active Galactic Nuclei or Gamma Ray Burst sources, characterized by a large product of the magnetic field times the acceleration length. They are able to produce jets of hadronic matter at least up to 10^{21} eV, and this huge acceleration of nucleons yields a photo-production of pions and thus a copious emission of neutrinos carrying some percent of the primary particle energy. According to the peculiar properties of the astrophysical sources the neutrino emission can be characterized or not by the simultaneous emission of UHE charged particles (thin or thick sources). The situation is much more simple for top-down models where the UHE particles are produced by the decay of massive relic particles, remnants of the Big Bang, and still present with some abundance in the cosmos. In this case, these relics decay into particle-antiparticle pairs and among the decay channels the ones producing neutrinos and photons are favoured. Since ν 's only interact weakly, once produced they can travel in the cosmos without significant energy loss and deflection. This is completely different from UHE charged particles or photons, which suffer an exponential flux reduction due to the Greisen-Zatsepin-Kuzmin (GZK) cut-off [3] and a variation of the arrival directions in presence of large diffused magnetic fields. Thus, even at this energy, one could observe a significant neutrino flux and do a reasonable neutrino astronomy.

In this framework, the new generation of cosmic ray surface detectors, like the Pierre Auger Observatory [4], and the neutrino telescopes, like Amanda [5], Icecube [6], Antares [7], and EUSO [8] will be able to study neutrinos of astrophysical origin in a wide range of energies. This will improve our understanding of the astrophysical acceleration mech-

anisms for bottom-up scenarios or, if top-down models were confirmed, will give new insights on fundamental interactions.

In the same way as the more usual components of cosmic radiation, also UHE ν 's can initiate EAS which could be detectable both by large surface and fluorescence detectors. Leaving apart vertical air showers, where the probability of a ν interaction with the ~ 1000 g/cm² of atmospheric depth is negligibly small, the best choice to look for a clear signature of neutrino induced events, studying EAS in array like AUGER, is the case of almost horizontal, skimming, or up-going air showers. In particular, neutrino air showers at large zenith angles, contrary to the proton ones [9], can be initiated deep in the atmosphere, producing both fluorescence yield in their longitudinal development and arriving to the ground detectors with a non attenuated electromagnetic component. These qualitative features of neutrino induced showers should however be supported by simulations, which are a necessary quantitative tool for the interpretation of the experimental data.

Neutrino detection in Auger has been previously addressed [10, 11], and some solution has been adopted [11] for the simulation of ν induced showers. In this respect, one has to take into account that none of the official Monte Carlo's used by the collaboration for shower simulation in atmosphere, CORSIKA [12] and AIRES [13], treats neutrinos as primary particles. Therefore, the authors in [11] used AIRES for simulating the interaction of muon neutrinos, injecting at low altitudes protons with a fraction of the energy of the initial neutrinos, accompanied by a photon shower in the case of an electron neutrino. Our approach in this framework is, instead, to extend the capabilities of a tool like CORSIKA, already used by a large number of people in the cosmic ray community, with the inclusion of neutrinos to the (already long) list of primary particles which it can handle. In case of primary neutrinos, we make a call to an existing Monte Carlo, HERWIG [14], to treat only the neutrino first interaction, and then leave in the hands of CORSIKA the products of such interaction. The HERWIG event generator is continuously updated by particle physics community, which makes it an extremely reliable tool for the description of particle interactions. This represents the main advantage of our approach.

The paper is organized as follows: in sections 2 and 3 we describe the two Monte Carlo codes CORSIKA and HERWIG, respectively. The modified version of the shower gener-

ator is outlined in section 4, whereas in section 5 we report the results of our simulation and in section 6 give our conclusions.

2 CORSIKA Monte Carlo

CORSIKA (COsmic Ray SImulations for KAscade) [12] is a detailed Monte Carlo program to study the EAS in the atmosphere initiated by photons, protons, nuclei and many other particles. It was originally written to perform simulations for the Kascade experiment [15], but during the time it became a tool which is used by many groups and its applications range from Cherenkov telescope experiments ($E_0 \sim 10^{12}$ eV) up to giant cosmic ray surface experiments at the highest energies observed ($E_0 > 10^{20}$ eV).

The most serious problem of EAS simulation programs is the extrapolation of the hadronic interaction to higher energies and into rapidity ranges which are not covered by experimental data. In particular, the extreme forward direction is not accessible by present collider experiments, but the particles in this kinematical region play the more important role in the development of EAS. In fact, they are the most energetic secondary particles which carry deep in the atmosphere the largest energy fraction of each collision. Therefore one has to rely on extrapolations based on theoretical models.

The simplest hadronic model, HDPM, was produced in the 1989 by Capdevielle [16] and inspired by the Dual Parton Model [17]. It describes the hadronic interactions of protons at high energies in good agreement with the measured collider data. As an alternative to the phenomenological HDPM generator one can use other hadronic interaction models. VENUS [18], QGSJET [19], and DPMJET [20] describe the inelastic hadronic interaction in the theoretically well founded Gribov-Regge [21] theory of multi-Pomeron exchange, which has been successfully used over decades for treating elastic and inelastic scattering of hadrons. SIBYLL [22] instead is a minijet model that describes the rise of cross-section with energy by increasing the pairwise minijet production. Particle tracking with ionization and radiation losses, multiple scattering and decay of unstable particles are performed for all models in the same way. In the last version of CORSIKA the new model NEXUS [23] has been added, which combines algorithms of VENUS and QGSJET with ideas based on the data from the experiments H1 and ZEUS, and is best suited

for extrapolations up to higher energies. Further, the GHEISHA routines [24] have been introduced to have a more sophisticated treatment of low energy hadronic interactions with respect to the old ISOBAR model. In fact, the hadronic models are only used for reactions above $E_{lab} = 80$ GeV/N, and below this threshold the GHEISHA code is used or the recently added UrQMD program [25], designed to treat low energy hadron-nucleus and nucleus-nucleus interactions.

In contrast to the hadronic particle production, the electromagnetic interactions of shower particles can be calculated very precisely from Quantum Electrodynamics. Therefore electromagnetic interactions are not a major source of systematic errors in the shower simulation. Very well tested packages exist to simulate these reactions in great detail, like EGS4. CORSIKA uses an adapted version of EGS4 for the detailed simulation of electromagnetic interactions, which includes the Landau-Pomeranchuk-Migdal [26] effect, the production of muon pairs and hadrons by photons, muon bremsstrahlung and $e^+ + e^-$ pair production by muons. EGS was also modified to accommodate the changes in the atmospheric density and to compute particle production with double precision, following the particles up to energies of typically 100 keV. In addition, the total energy deposited along the shower axis is recorded, all two and three body decays, with branching ratios down to 1%, are modelled in a kinematically correct way, and particle tracking and multiple scattering are realized in great detail. An alternative way of treating the electromagnetic component is to use the improved and adapted form of the analytical NKG formula [27] for each electron or photon produced in the hadronic cascade. Last but not least, to account for seasonal and geographical variations CORSIKA allows the choice of a variety of atmospheric density profiles and the definition of new ones.

The CORSIKA program recognizes more than 50 elementary particles:

- $\gamma, e^\pm, \mu^\pm;$
- $\pi^o, \pi^\pm, K^\pm, K_{S/L}^o$ and $\eta;$
- the baryons $p, n, \Lambda, \Sigma^\pm, \Sigma^o, \Xi^o, \Xi^-, \Omega^-$ (and the corresponding antibaryons);
- the resonance states $\rho^\pm, \rho^o, K^{*\pm}, K^{*o}, \bar{K}^{*o}, \Delta^{++}, \Delta^\pm, \Delta^o$ (and the corresponding antibaryonic resonances);

- nuclei up to $A \leq 56$.

Concerning neutrinos, the ν_e 's and ν_μ 's and the corresponding antineutrinos produced in π , K and μ decays, may be generated explicitly by using a particular option of CORSIKA, but they cannot be chosen as primary particles. However, as discussed in the introduction, atmospheric showers induced by neutrinos arriving to earth are of great interest from different points of view. Here, it is worth pointing that neutrino fluxes, at the origin expected with the ratios $\nu_e : \nu_\mu : \nu_\tau = 1 : 2 : 0$, would evolve towards the ratios $1 : 1 : 1$ due to oscillations. Therefore, the inclusion of all neutrino flavours in the list of primaries of CORSIKA could be very helpful to the aim of exploring a large class of phenomena in cosmic ray physics.

3 HERWIG Monte Carlo

HERWIG [14] is an event generator for high-energy processes particularly suited for detailed simulation of QCD parton showers. It provides simulation of hard lepton-lepton, lepton-hadron and hadron-hadron scattering and soft hadron-hadron collisions within a single package.

The main features of HERWIG are:

- use of angular ordering to account for initial and final-state jet evolution in QCD with soft gluon interference;
- color coherence of (initial and final) partons in all hard subprocesses, including the production and decay of heavy quarks and supersymmetric particles;
- azimuthal correlations within and between jets due to gluon interference and polarization;
- jet hadronization via cluster formation based on non-perturbative gluon splitting, and a similar cluster model for soft and underlying hadronic events;
- a space-time picture of event development, from parton showers to hadronic decays, with an optional colour rearrangement model based on space-time structure.

The main features of a hard process (with high momentum transfer) simulated by HERWIG can be grouped in the following four classes, presented in order of increasing scales of distance and time:

1. Elementary hard subprocess. Two beam particles, or their constituents, interact and produce one or more outgoing fundamental objects. The boundary conditions for the initial and final-state parton showers are chosen by using the hard scale of the momentum transfer, Q , and the color flow of the subprocess.
2. Initial and final-state parton showers. A parton constituent of an incident hadron with low space-like virtuality can radiate time-like partons. On a similar time scale, an outgoing parton with large time-like virtuality can generate a shower of partons with lower virtuality. Moreover, partons from the initial-state emission can produce parton shower. The actual amount of emission is again controlled by the momentum transfer scale of the hard subprocess, Q .
3. Heavy object decay. Massive object (top quarks, higgs bosons, etc.) can decay on time scales shorter or comparable to that of the QCD parton showers. Depending on their decay mode, they can also produce parton showers before or after decaying.
4. Hadronization process. As a last step, to produce a realistic simulation one has to combine the partons into hadrons. This hadronization process takes place at low momentum transfer scale, where α_s is large and perturbation theory is not applicable. Nevertheless, these kind of processes can be described by phenomenological models. In HERWIG this is made by terminating showering at a low scale, $Q_0 < 1$ GeV, where colour neutral clusters are formed, which decay into the observed hadrons. Initial-state partons are incorporated into the incoming hadron through a soft non perturbative “forced-branching” phase of space-like showering. Instead, constituent spectator partons participate in a soft “underlying event” interaction, modelled on soft minimum bias hadron-hadron collisions.

The version 6.5 of HERWIG is presently available and is planned to be the last release in Fortran. Future developments, to be released in 2003, will be implemented using C++ [28].

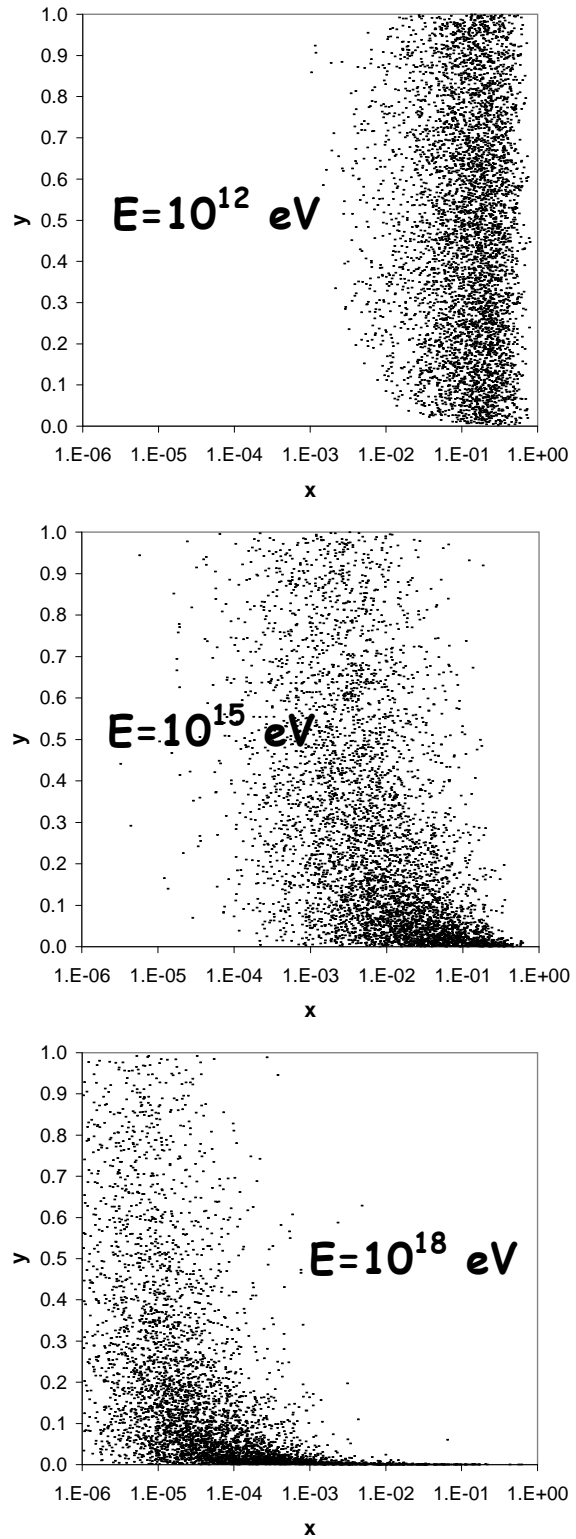


Figure 1: Distribution in the space of the Bjorken invariant variables x and y , of 5000 $\nu_\mu + p \rightarrow \mu^- + X$ events. From top to bottom the neutrino energy is 10^{12} , 10^{15} , and 10^{18} eV.

For the present analysis we adopted HERWIG 6.4, which uses standard Fortran 77. With this code a preliminary study of the first interaction of a neutrino on a nucleon $\nu(k) + N(p) \rightarrow l/\nu(k') + X(p')$ was performed. As far as the structure of events in phase space is concerned, in Fig. 1 we show, for a ν_μ Charge Current (CC) interaction at $E_{\nu_\mu} = 10^{12}$, 10^{15} , and 10^{18} eV, the distribution of events in the space of the Bjorken variables

$$x \equiv \frac{-q^2}{2 p \cdot q} \equiv \frac{Q^2}{2 p \cdot q}, \quad (3.1)$$

$$y \equiv \frac{p \cdot q}{p \cdot k}. \quad (3.2)$$

In the above equations $q = k - k'$ is the momentum transfer to the nucleon. The x variable represents the fraction of the parent nucleon momentum carried by the incoming parton, while in the nucleon rest frame $y = 1 - E_l/E_\nu$ is connected to the fraction of neutrino energy to the outgoing lepton. Fig. 1 shows that neutrinos with higher energies probe the Parton Distribution Functions (PDF's) inside the nucleon at lower x . At the same time, the rise of E_ν results in a larger fraction of the primary energy to the outgoing lepton, $E_l/E_\nu = 1 - y$. This is better seen in Fig. 2 (upper plot), where one can see the spectrum of the outgoing lepton resulting from the same events shown in Fig. 1. Lower plot in Fig. 2 shows that the outgoing lepton produced in the first interaction of the neutrino carries away more than 90% of the neutrino energy in 10% of the cases at $E_\nu = 10^{12}$ eV, but this percentage increases to 37% at $E_\nu = 10^{15}$ eV and to 54% at $E_\nu = 10^{18}$ eV. Note that the above features of Fig. 1 and Fig. 2 are encoded in the particular dependence of the $\nu - N$ cross-section on x and y .

It is also worth noticing that the default PDF's used by HERWIG, the MRST Leading Order PDF's [29], are valid in the ranges $x \geq 10^{-6}$ and $1.25 \text{ GeV}^2 \leq Q^2 \leq 10^7 \text{ GeV}^2$. This means that one needs extrapolations of the PDF's only for energies of the incoming neutrino $\gtrsim 10^{18}$ eV, which are much larger than the values we have considered in this analysis.

Last but not least, we have studied the typical particle population of an event simulated by HERWIG. At this aim we have selected, from the output of the Monte Carlo, the produced First Interaction (FI) particles. The average number of a given particle type is

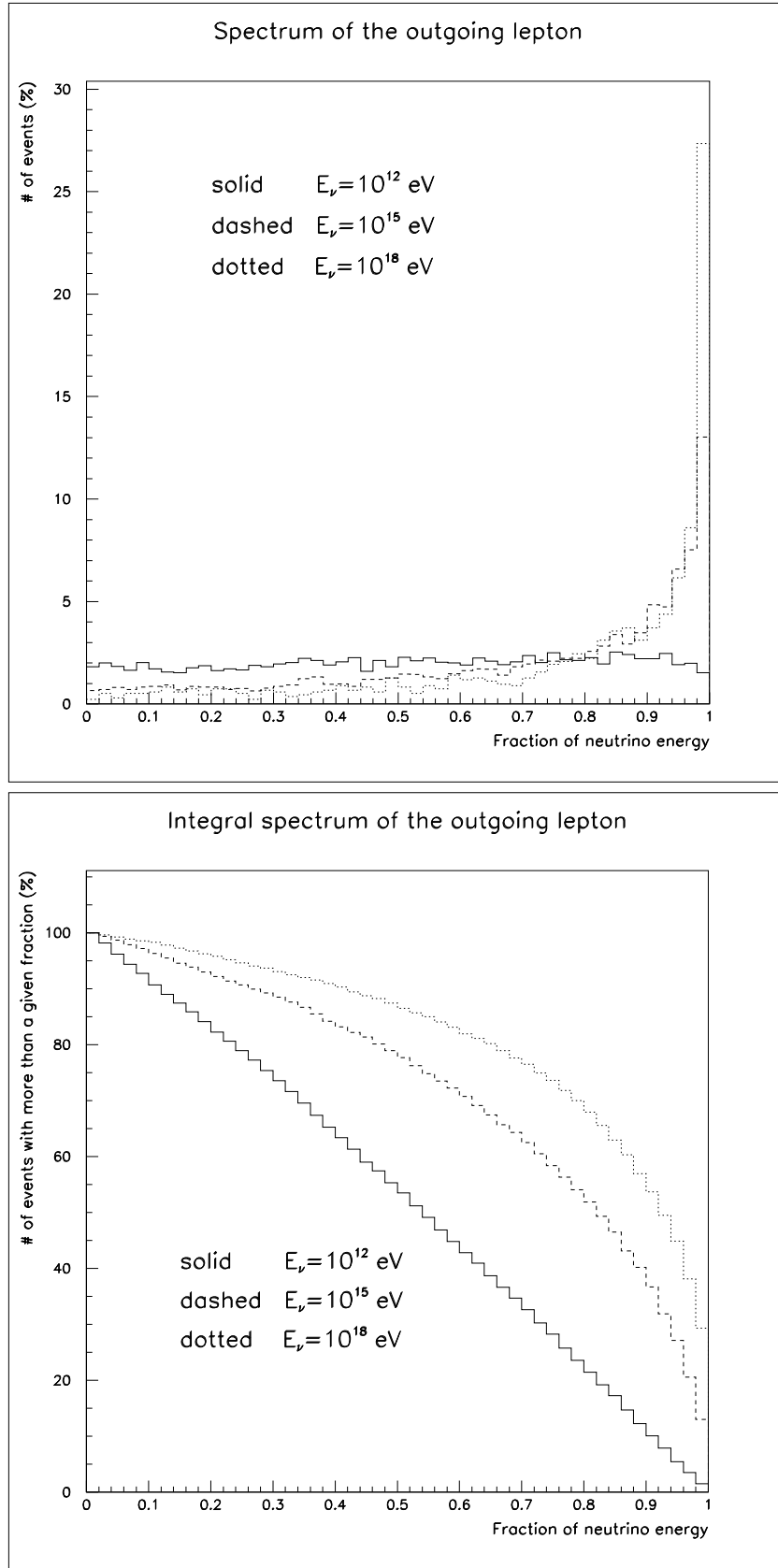


Figure 2: Spectrum of the outgoing lepton for the same events showed in Fig. 1. Upper (lower) plot shows the number of events with a given fraction (the number of events with more than a given fraction) of the neutrino energy to the outgoing lepton.

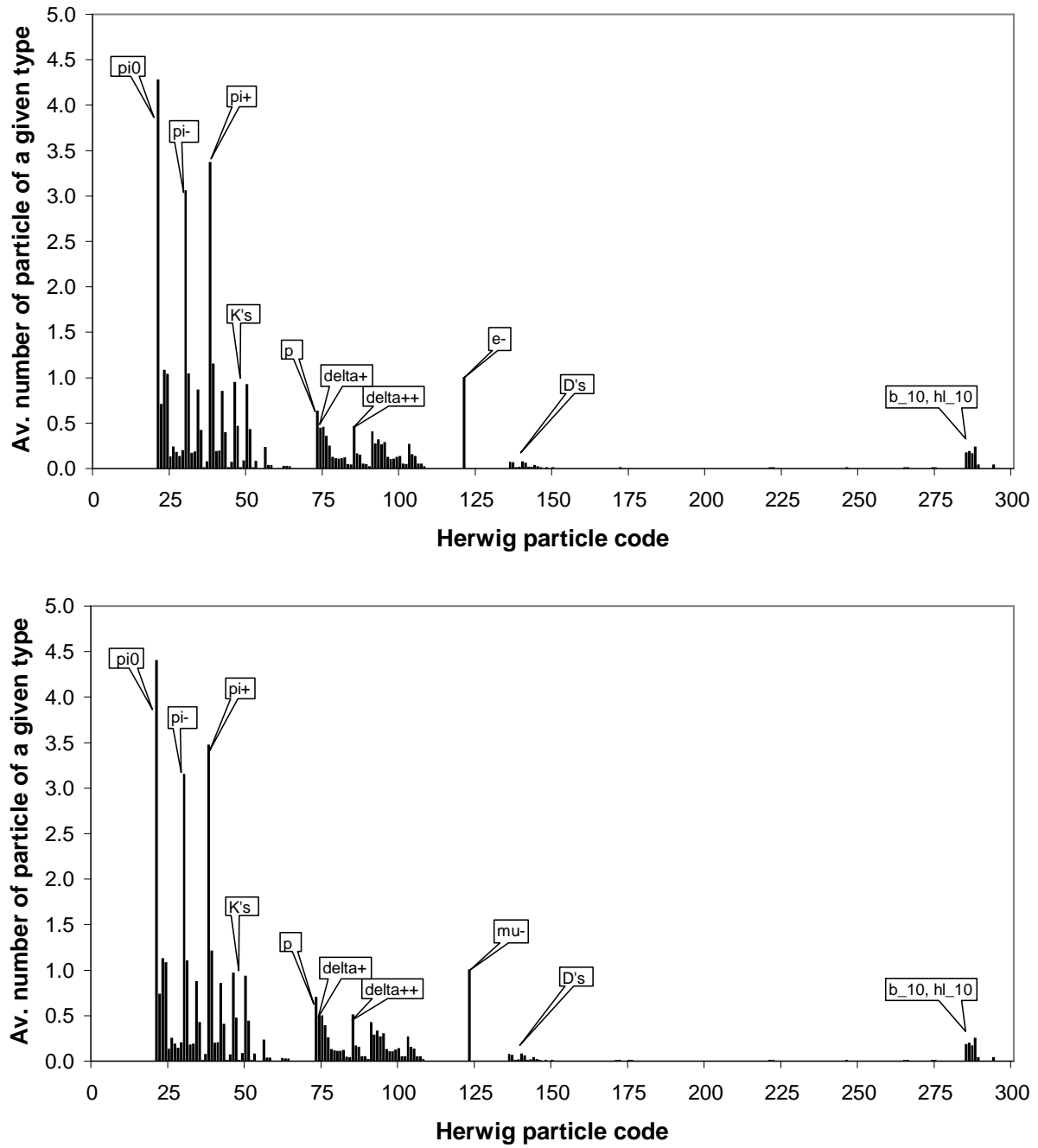


Figure 3: Average numbers of different particle types produced in the processes $\nu_e + p \rightarrow e^- + X$ (upper plot) and $\nu_\mu + p \rightarrow \mu^- + X$ (lower plot) at $E_\nu = 10^{15}$ eV.

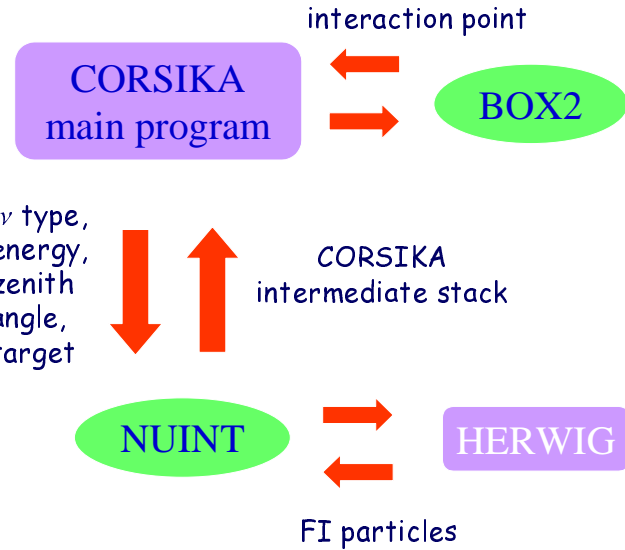


Figure 4: Flow diagram of the neutrino modified version of CORSIKA.

shown in Fig. 3 for ν_e and ν_μ at $E_\nu = 10^{15}$ eV. From the plots it is clear that, together with ordinary particles like π 's, K 's, N 's, and Δ 's, some other species are produced which are not yet recognized by CORSIKA (like charmed particles). However, this problem can be overcome at the energies of interest for the present analysis, as we will see in the next section.

4 A modified version of CORSIKA for neutrino simulation

For the present work we used the CORSIKA version 6.014, making our changes on the Fortran file extracted from the *.car* source by using the software CMZ [30]. In the extraction, we used HDPM as the hadronic interaction model, EGS4 for describing the electromagnetic interactions, and the CURVED atmosphere option. The choice of HDPM is due to the fact that this model is the simplest among the hadronic ones available in CORSIKA, even if it agrees with experimental data only up to the energies of $\sim 10^{16}$ eV. This motivated our choice of $E_{primary} = 10^{15}$ eV for the simulations on which the present analysis is based.

The implementation of the neutrino modified version of CORSIKA consists of two main steps, as showed in the flow diagram in Fig. 4. The first one is a modification in

the subroutine BOX2, where the interaction point of any particle is calculated, and the second one is a change in the main program, for generating the first interaction of the primary particle.

Actually, the first modification was made only for completeness, since the cross-section of neutrino interaction with matter is so small that, even in the case of the largest zenith angles of the primary neutrino, meaning a crossed column depth of ~ 36000 g/cm², the probability of producing a shower is very small. Due to this, we always asked CORSIKA to make the neutrino first interaction at a fixed height. In any case, in view of future implementations of the neutrino first interaction to higher energies, in BOX2 the neutrino cross-section quoted in [31] can be used, that is

$$\sigma_{tot}(\nu N) = 7.84 \cdot 10^{-36} \text{ cm}^2 \left(\frac{E_\nu}{1 \text{ GeV}} \right)^{0.363}, \quad (4.3)$$

$$\sigma_{tot}(\bar{\nu} N) = 7.80 \cdot 10^{-36} \text{ cm}^2 \left(\frac{E_\nu}{1 \text{ GeV}} \right)^{0.363}, \quad (4.4)$$

which have 10% accuracy within the energy range 10^{16} eV $\leq E_\nu \leq 10^{21}$ eV.

As far as the second change is concerned, we inserted in the main program a conditional call to a link subroutine, NUINT, executed only for a primary neutrino and in the first interaction case. In this subroutine, the necessary quantities for making the call to the HERWIG event generator are generated from the input quantities, that is the neutrino type¹ ($\nu_e, \bar{\nu}_e, \nu_\mu, \bar{\nu}_\mu$), its energy and zenith angle, and the target nucleon. This is chosen randomly between a proton or a neutron, and the process, CC or Neutral Current (NC) deep inelastic scattering, is selected by using the comparison of the respective cross-sections [31],

$$\sigma_{CC}(\nu N) = 5.53 \cdot 10^{-36} \text{ cm}^2 \left(\frac{E_\nu}{1 \text{ GeV}} \right)^{0.363}, \quad (4.5)$$

$$\sigma_{NC}(\nu N) = 2.31 \cdot 10^{-36} \text{ cm}^2 \left(\frac{E_\nu}{1 \text{ GeV}} \right)^{0.363}, \quad (4.6)$$

$$\sigma_{CC}(\bar{\nu} N) = 5.52 \cdot 10^{-36} \text{ cm}^2 \left(\frac{E_\nu}{1 \text{ GeV}} \right)^{0.363}, \quad (4.7)$$

$$\sigma_{NC}(\bar{\nu} N) = 2.29 \cdot 10^{-36} \text{ cm}^2 \left(\frac{E_\nu}{1 \text{ GeV}} \right)^{0.363}. \quad (4.8)$$

¹Tau neutrino were not considered in this analysis since their charged current interaction would have produced a tau lepton which, in the 6.014 version of CORSIKA, is not handled by the program. On the other side, its treatment with HERWIG would have gone beyond the aims of this study.

The call to HERWIG is made in a standard way (see, for example, a sample main program at the HERWIG home page [32]). We select the first *good* event from a total of MAXEV=100. This means that, in the user's routine for terminal calculations (in [32] this routine is called HWAEND) several checks are made before accepting the event: a) the event is discarded if the total energy of the daughter FI particles differs by more than 1% from the primary neutrino energy; b) the event is discarded if the values of the invariant variables which describe the deep inelastic process, x and Q^2 , are out of the ranges where the PDF's are given². In this respect, we used the MRST Leading Order PDF's [29], which are the default PDF's in HERWIG.

When selecting from the output of HERWIG the FI particles, we have to face a difficulty: the typical zoo of FI particles we obtain (see Fig. 3) can, and actually does in most of the cases, include some products which are not present in the list of particles recognized by CORSIKA. At the energy we have chosen for this analysis, $E_\nu = 10^{15}$ eV, the average fraction of events with more than 10% of the primary energy in these unrecognized products is $\sim 31\%$. On the other side, the γ factor of these particles at this energy is such that they would not cover a very long distance in the atmosphere, and an acceptable solution to the problem is to substitute them directly with their decay products. This is made inside the routine HWAEND, where, once determined that the current particle is not among the ones treated by CORSIKA, it is replaced with its daughter particles already produced by HERWIG.

Once the FI particles have been selected, the array SECPAR of CORSIKA, filled in the routine HWAEND with all the information about the current particle, is used for transferring them to the CORSIKA intermediate stack STACKINT (these particles are then transferred by CORSIKA to the real stack, STACK, and then written to the output file).

Besides the changes we have described, some other minor modifications were made, concerning the data sent to the output, for collecting all the information on the neutrino first interaction.

²Strictly speaking, this would imply a bias against values favoured by the cross-section but out of the present acceptable ranges of x and Q^2 . However, at the energy we are concerned, the cross-section is dominated by x and Q^2 values in the accepted ranges (see middle plot in Fig. 1).

5 Results

With the new neutrino version of CORSIKA we generated a series of 30 showers for each neutrino species ($\nu_e, \bar{\nu}_e, \nu_\mu, \bar{\nu}_\mu$), 10 for each zenith angle in the set $\theta = 70^\circ, 75^\circ, 80^\circ$. These inclinations are such that one has to use the option of curved atmosphere in CORSIKA. The energy of the primary ν was $E_\nu = 10^{15}$ eV. At the same time, we produced, with the version 6.014 of CORSIKA, a correspondent set of proton showers with the same inclinations and primary energy. In order to make the comparison between the two class of showers, the neutrino first interaction was realized at the same point of the corresponding proton shower (note that, on the contrary, the proton first interaction is driven by CORSIKA according to the proton-air cross-section). The observation level was chosen in such a way that an EAS with zenith angle $\theta = 70^\circ$ is intercepted at an atmospheric depth of 760 g/cm^2 . This situation is very similar to what occurs at the Auger level for the same particles but with a rescaled energy larger than 10^{18} eV. Changing the inclination of the primary to $\theta = 75^\circ$ and 80° the observation level correspondingly moves to a depth of 1005 and 1497 g/cm^2 , respectively.

We analyzed each set of 10 showers at a given primary zenith angle in order to obtain an average behaviour. The results are showed in Figs. 5-11. We show in Fig. 5 the comparison of the longitudinal profiles of charged particles versus the slant atmospheric depth for proton, electron and muon neutrinos and antineutrinos at $\theta = 70^\circ$. From this plot, no significant difference between neutrinos and antineutrinos of the same type is appreciable. This feature results to be independent of the shower inclination, and hence hereafter the plots for antineutrinos will be omitted. For muon neutrinos the particle number at the maximum is lower than for protons, while for electron neutrinos is larger. This has a unique explanation in terms of the outgoing lepton spectrum. In fact, for $E_\nu = 10^{15}$ eV the outgoing lepton produced in the first interaction of the neutrino carries away more than 90% of the neutrino energy in 37% of the cases (see Fig. 2). In this respect it is worth noticing that, for a given inclination, each set of 10 ν_μ showers has been produced by using the same seeds of the corresponding ν_e ones; consequently, the outgoing lepton energy distribution is the same, as well as the percentage of CC events

with respect to NC ones³. The energy of the outgoing lepton does not contribute to the development of the shower, and is then undetectable, either for a neutrino NC interaction or for a muon neutrino CC one which produces a very energetic muon hitting the ground at the core shower. On the other side, a CC interaction of a ν_e in most of the cases produces an electron with a large fraction of primary energy, and less energetic hadronic products. From these first interaction particles a mixed shower is generated, partly electromagnetic and partly hadronic. By increasing the energy fraction delivered to the electron, the electromagnetic features of this shower become dominant with respect to the hadronic ones. In this case the rise in the number of charged particles (predominantly electrons and positrons) stops later, since the critical energy in an electromagnetic shower is lower than in a hadronic one. This is confirmed in Fig. 6, where the showers initiated by a proton and an electron neutrino (with an energy fraction to the secondary electron of 99% and 2%, respectively) are plotted for $\theta = 70^\circ$, and compared to a corresponding 10^{15} eV electron shower⁴. When the FI electron in the ν_e shower takes 99% of the neutrino energy the height of the e and ν_e longitudinal peaks are comparable, while when the fraction of neutrino energy to the FI electron is 2% the height of the maximum in the ν_e longitudinal profile is similar to the proton one.

In Fig. 7 the longitudinal developments at $\theta = 70^\circ$, 75° and 80° are shown for ν_e and ν_μ primaries. In principle, the average longitudinal profile of charged particles versus the slant depth should not depend on the zenith angle. However, if the average, as in our case, is performed on a small number of simulations one has to take into account the Monte Carlo fluctuations. This is actually the reason for the different features of ν_e and ν_μ profiles at different angles reported in Fig. 7. The origin of these fluctuations is mainly twofold: the event can be CC or NC mediated and the energy of the outgoing lepton has the distribution showed in Fig. 2. In Fig. 8, in order to disentangle the two effects, we plot the ν_e average showers for $\theta = 70^\circ$, 75° and 80° , having separated the CC and NC first interaction events. The residual difference between the curves belonging to one

³The NC interaction has a cross-section which, in the interesting range of energies, is roughly an order of magnitude lower than the one for a CC one. Actually, in the set of 30 produced showers the fraction of events NC/(NC+CC) is 8/30 (1/10 for $\theta = 70^\circ$).

⁴This primary electron has been injected in the atmosphere at the point where the secondary electron is produced in the first interaction of the primary ν_e .

of the previous categories is due to the different energy fraction of the outgoing lepton, which is indicated in the plot. Note that, as expected, a smaller fraction of energy to the electron in the CC case (upper curves in Fig. 8) results in a decrease of the height of the maximum, while a smaller fraction to the electron neutrino in the NC case (lower curves in Fig. 8) amounts to an increase.

As pointed out in Ref. [33], the charged particle energy deposit is a quantity which is directly connected to the fluorescence yield produced in the longitudinal development of a shower. Actually, the authors of Ref. [33] note a good agreement between the shapes of the energy deposit and the charged particle profile. This is due to the ionization energy loss per particle, which is not much dependent on the energy. As a consequence, for slant depth ≥ 300 g/cm², the two curves differ for a mere multiplicative factor (see Fig. 7 in [33]). The comparison between the energy deposit for proton, ν_e and ν_μ induced showers, at $\theta = 80^\circ$, is reported in Fig. 9. As shown in this graph, the CC ν_e curve is much higher than the NC ν_e and ν_μ curves, since in both the last cases the outgoing lepton does not produce further ionization. This implies that, at least for a primary energy of $\sim 10^{15}$ eV, the threshold for the detection of a CC ν_e shower by fluorescence is lower than for a NC ν_e or a ν_μ one. On the other side, Fig. 10 shows the dependence on the zenith angle of the energy deposit for ν_e and ν_μ induced showers.

Finally in Fig. 11 the lateral distributions of charged particles versus the distance from the shower axis for p , ν_e , and ν_μ induced showers at $\theta = 70^\circ$ are plotted. The curves confirm the clear differences already noted between the showers induced by the two neutrino flavours.

6 Conclusions and outlook

In this paper we have described the results obtained by a modified version of CORSIKA, accounting also for neutrinos as primary particles. This tool uses a call to the HERWIG Monte Carlo to implement the first interaction of the neutrino. The analysis of the simulated showers for a primary energy of 10^{15} eV suggests that the longitudinal profile of EAS induced by ν_e 's is sensibly enhanced with respect to the corresponding proton showers. On the contrary a large suppression of the profile is observed for primary ν_μ 's.

As a consequence of this, the threshold for ν_e shower detection both for the surface array and the fluorescence detection is lower than for the proton one, while for ν_μ is higher.

This suggests to better explore the possibility to discriminate between neutrino flavours by the fluorescence detector in the Auger experiment. In fact, since the depth of the maximum in the longitudinal development of a shower is directly related to the primary energy, it should be easy to single out ν_e induced showers with CC first interaction at energies lower than the threshold for detecting NC ν_e or ν_μ showers. Going to higher energies, an estimate of the NC ν_e or ν_μ shower contamination can be provided by considering the ratio between neutrino fluxes of different flavour and the probability of NC versus CC ν first interactions.

Future work aims to extend the capabilities of the modified neutrino version of CORSIKA to energies $\geq 10^{16}$ eV. In this range one is urged to substitute the simplified hadronic model HDPM with a more reliable one, like QGSJET. Moreover, the approach we used for handling unrecognized particle in CORSIKA is no longer applicable to these high energies, and a treatment of τ lepton, charmed particles and resonances states, whose interaction is not included in the present version of the Monte Carlo, is necessary. Care has to be taken also of the extrapolation of PDF's to high energy, which determine the value of neutrino cross-section in the ranges of interest for the Auger experiment. In fact, while the fraction of events out of the present acceptable ranges of x and Q^2 is 0.02% at $E_\nu = 10^{15}$ eV and 2% at $E_\nu = 10^{18}$ eV, it becomes $\sim 40\%$ at $E_\nu = 10^{21}$ eV. All these research lines are at the moment under investigation.

7 Acknowledgements

We would like to thank D. Heck and J. Knapp for valuable comments and suggestions.

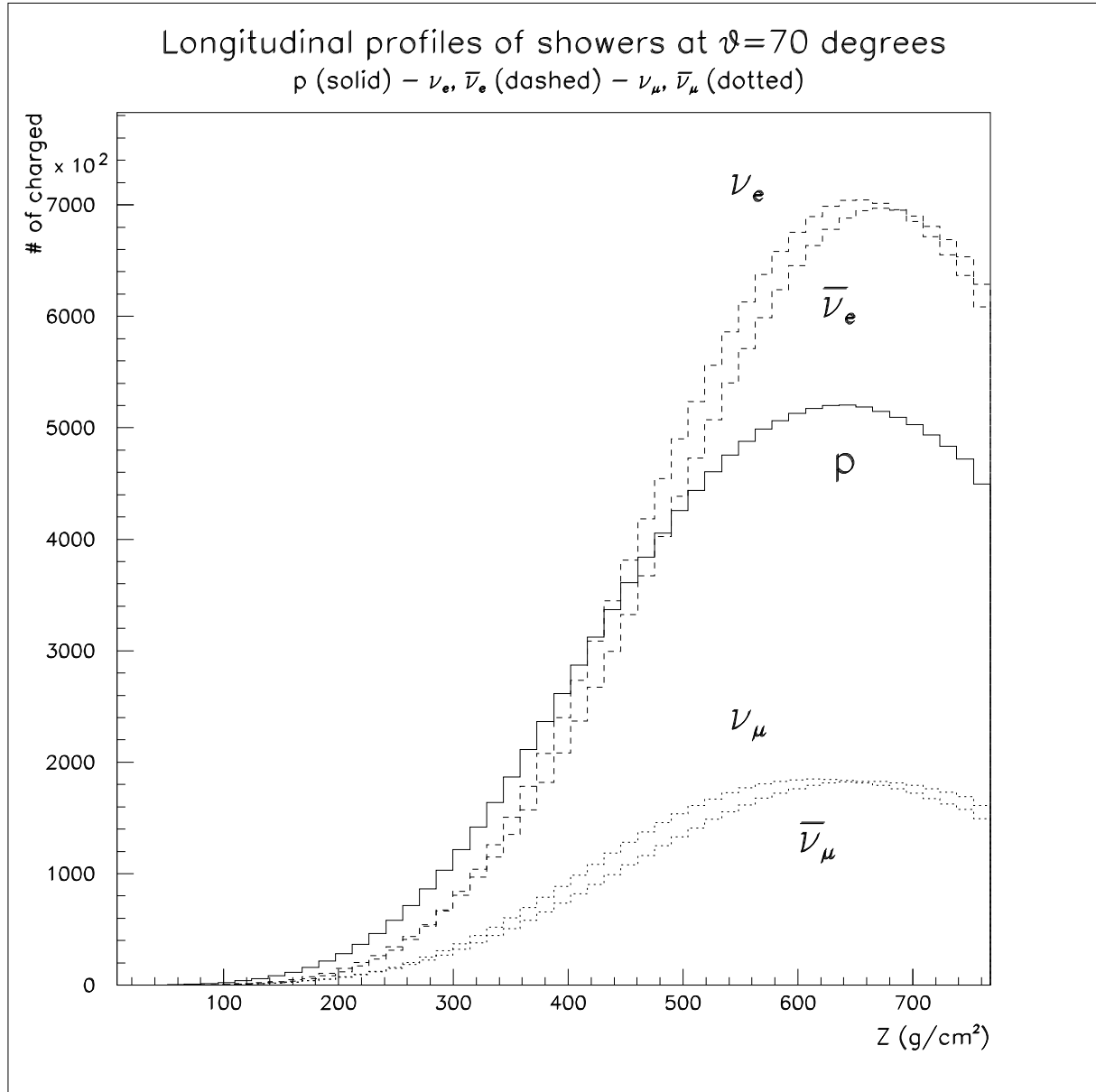


Figure 5: Average longitudinal profiles of showers induced by p (solid), ν_e and $\bar{\nu}_e$ (dashed), ν_μ and $\bar{\nu}_\mu$ (dotted) at the primary energy of 10^{15} eV and $\theta = 70^\circ$.

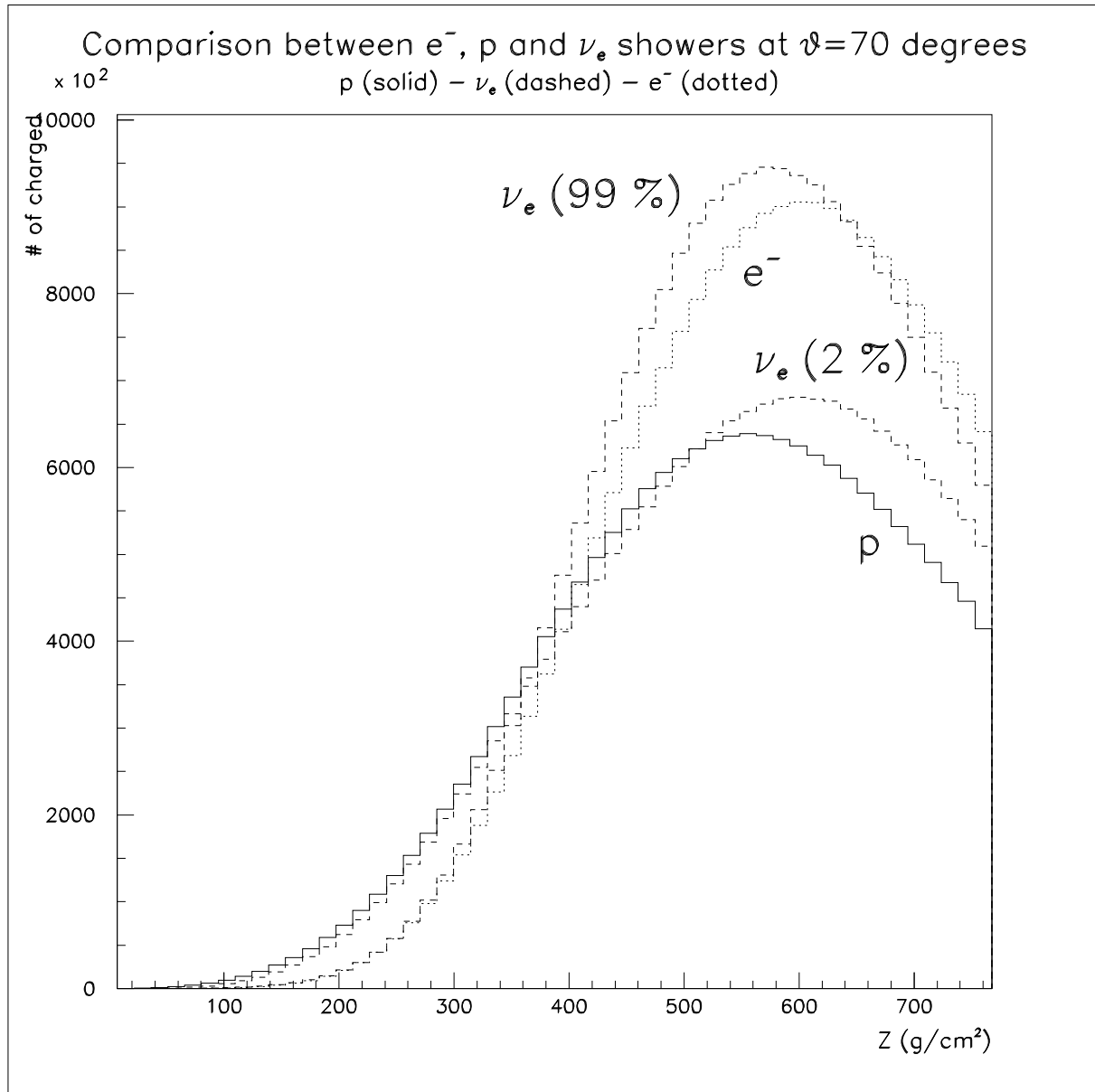


Figure 6: Comparison between the longitudinal profiles of showers induced by p (solid), ν_e (dashed), and e^- (dotted) with a primary energy of 10^{15} eV. The dashed curves correspond to ν_e showers with 99% and 2%, respectively, of the neutrino energy to the outgoing electron.

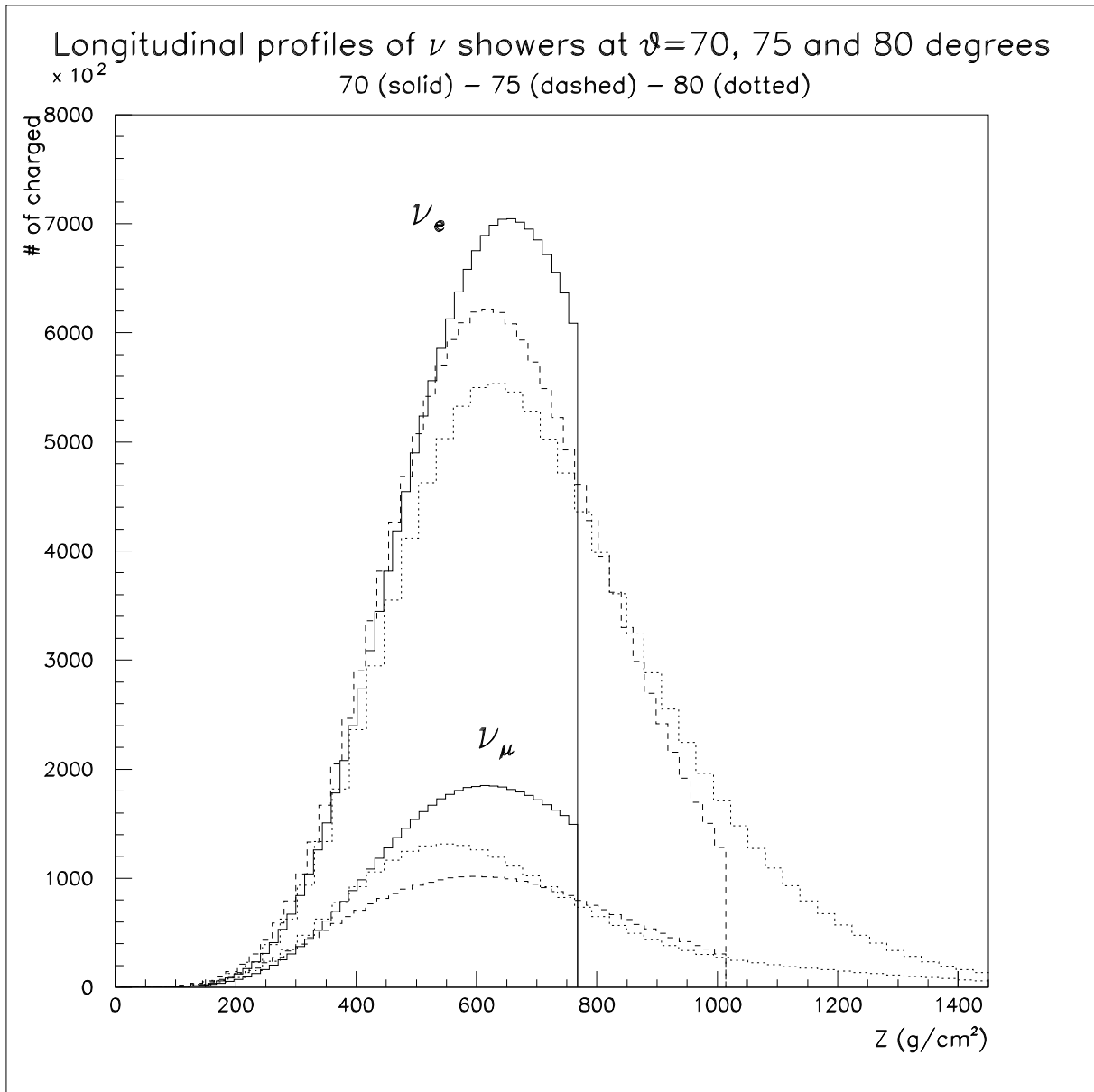


Figure 7: Average longitudinal profiles of showers induced by ν_e (upper curves) and ν_μ (lower curves) at the primary energy of 10^{15} eV and $\theta = 70^\circ$ (solid), 75° (dashed), and $\theta = 80^\circ$ (dotted).

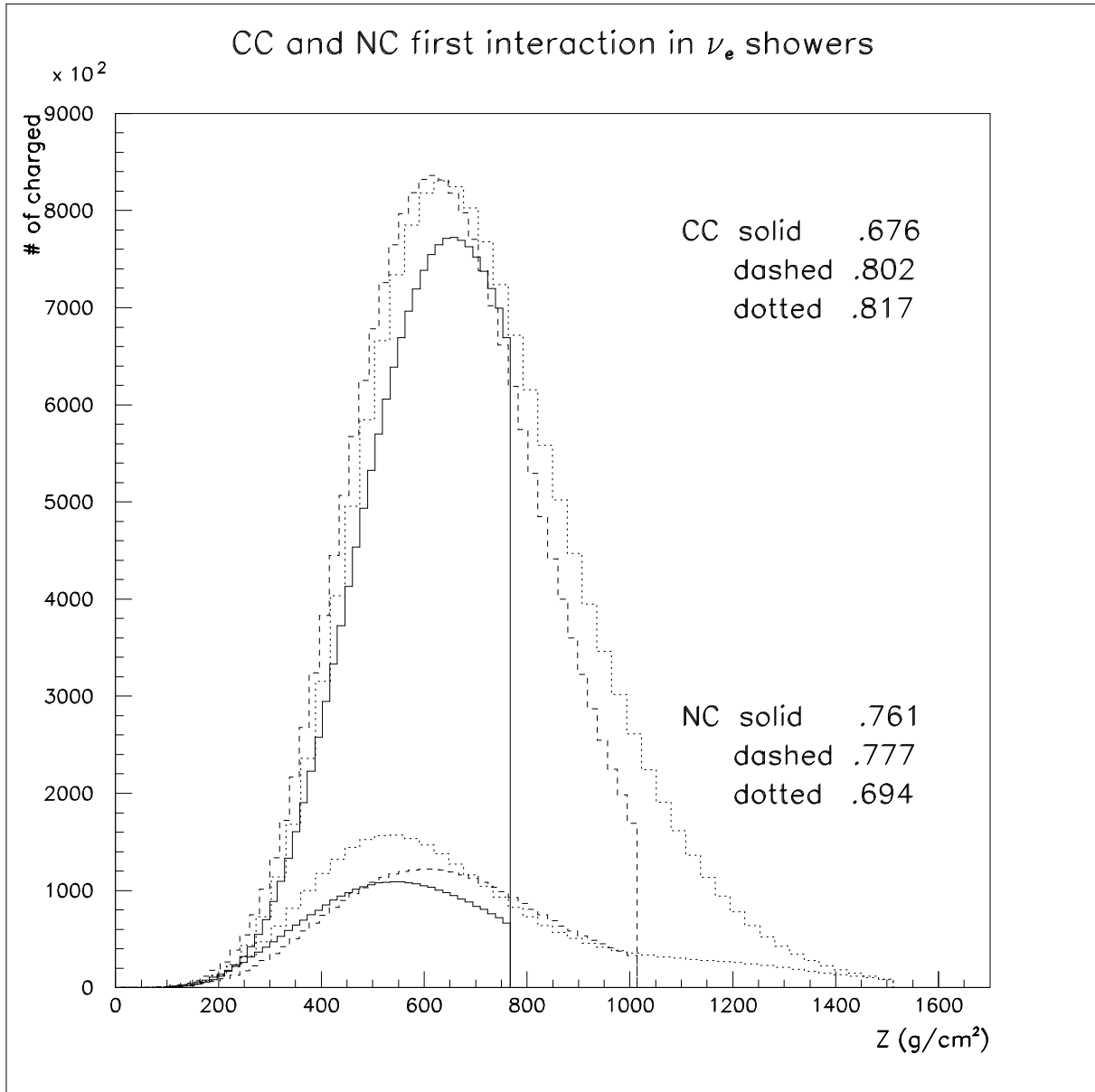


Figure 8: Average longitudinal profiles of showers induced by a ν_e developing a CC first interaction (upper curves) or a NC one (lower curves) at the primary energy of 10^{15} eV and $\theta = 70^\circ$ (solid), 75° (dashed), and 80° (dotted). The average fraction of the primary energy delivered to the secondary lepton is reported for each curve.

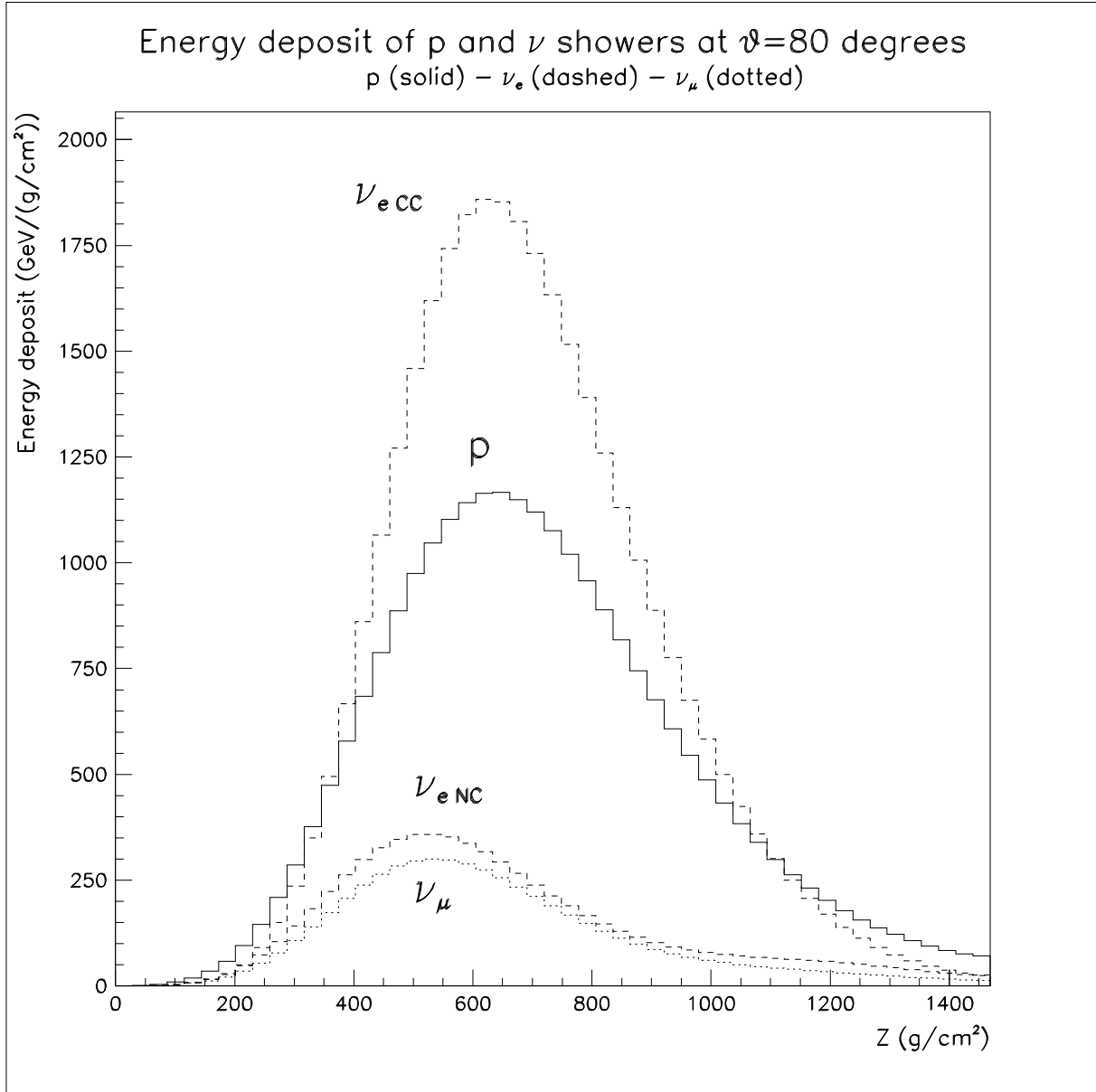


Figure 9: Comparison of the average energy deposit for showers induced by p (solid), ν_e (dashed) and ν_μ (dotted) at the primary energy of 10^{15} eV and $\theta = 80^\circ$. For ν_e the CC and NC average components are shown separately.

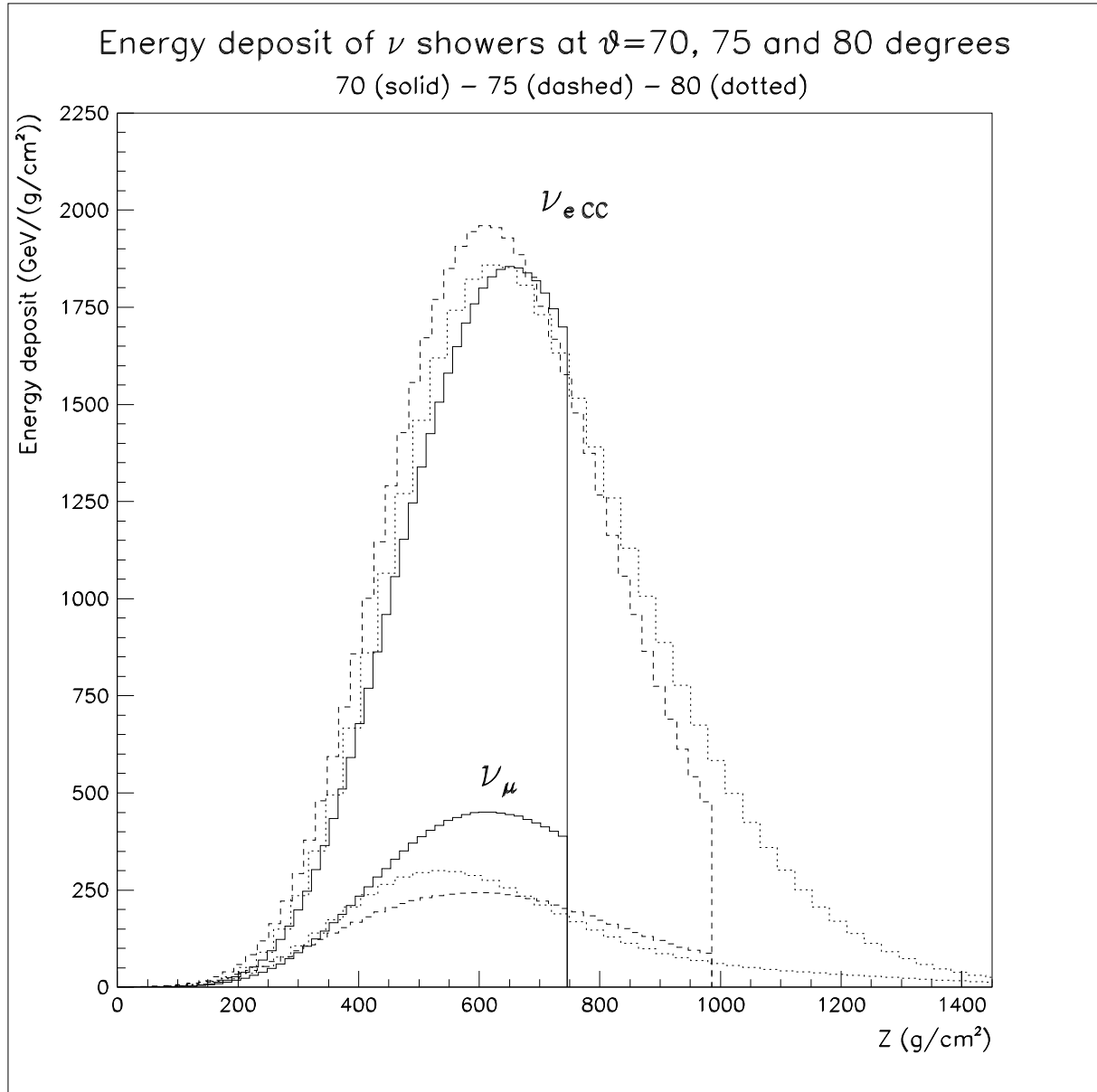


Figure 10: Comparison of the average energy deposit for showers induced by ν_e (CC component) and ν_μ at the primary energy of 10^{15} eV and $\theta = 70^\circ$ (solid), 75° (dashed), and 80° (dotted).

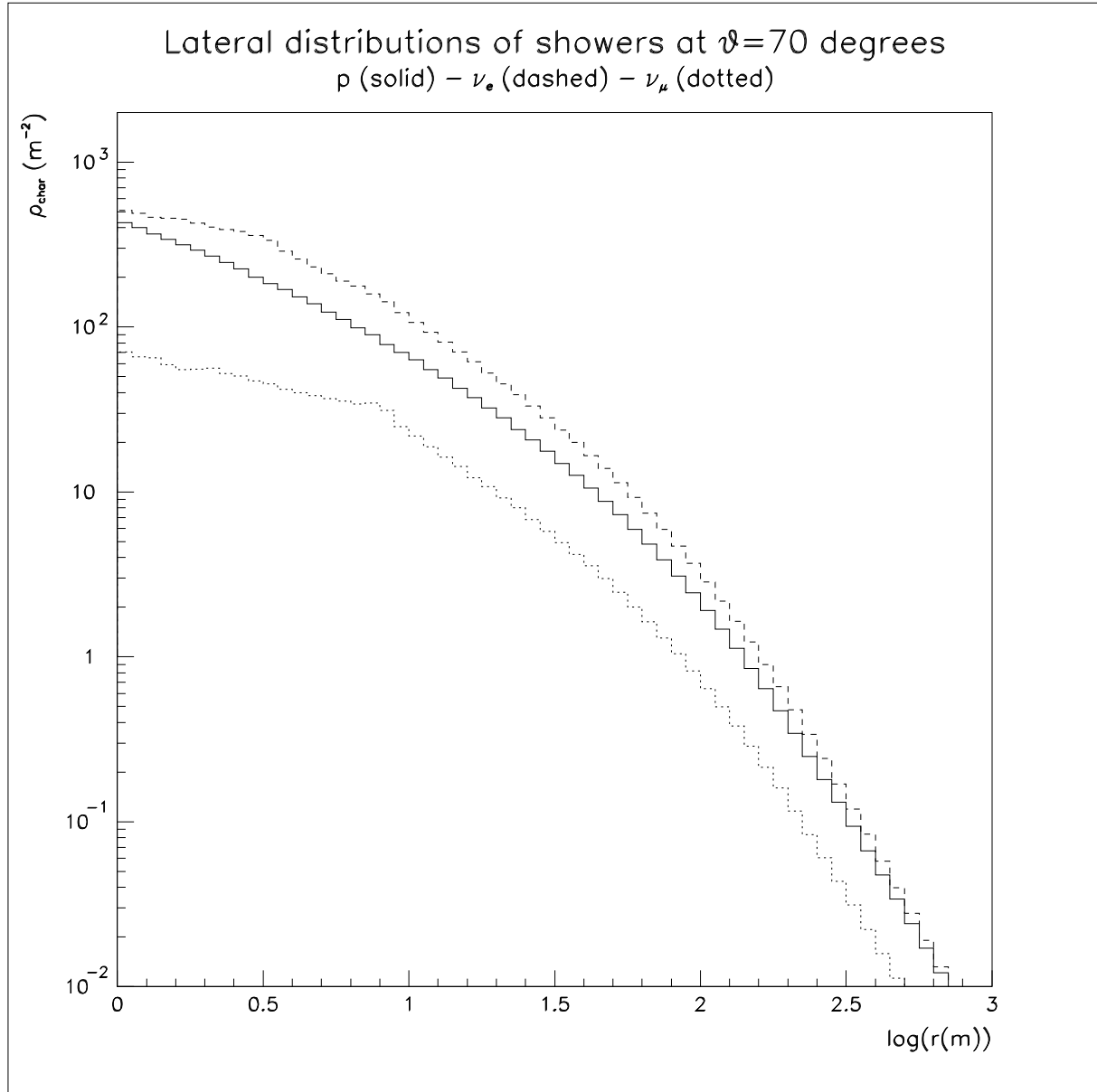


Figure 11: Average lateral density distributions of charged particles versus the distance from the shower axis at a slant depth of 760 g/cm^2 for the showers induced by p (solid), ν_e (dashed) and ν_μ (dotted) at the primary energy of 10^{15} eV and $\theta = 70^\circ$.

References

- [1] Volcano Ranch: J. Linsley, *Phys. Rev. Lett.* **10**, 146 (1963); Haverah Park: M.A. Lawrence, R.J.O. Reid, and A.A. Watson, *J. Phys. G: Nucl. Part. Phys.* **17**, 733 (1991); Fly's Eye: D.J. Bird et al., *Astrophys. J.* **441**, 144 (1995); Yakutsk: B.N. Afnasiev et al., *Proc. Int. Symp. on Extremely High Energy Cosmic Rays: Astrophysics and Future Observatories*, 32 (1996), ed. M. Nagano, Tokyo; AGASA: M. Takeda et al., *Phys. Rev. Lett.* **81**, 1163 (1998) and astro-ph/0209422, N. Hayashida et al., astro-ph/0008102; HiRes: T. Abu-Zayyad et al., astro-ph/0208243 and astro-ph/0208301.
- [2] G. Sigl, astro-ph/0210049.
- [3] K. Greisen, *Phys. Rev. Lett.* **16**, 748 (1966); G.T. Zatsepin and V.A. Kuzmin, *Pis'ma Zh. Eksp. Teor. Fiz.* **4**, 114 (1966) [*JETP. Lett.* **4**, 78 (1966)].
- [4] The Pierre Auger Observatory - Design Report, March 1997; P. Privitera for the Auger Collaboration, *Nucl. Phys. Proc. Suppl.* **110**, 487 (2002) (web page: <http://www.auger.org>).
- [5] P.C. Mock et al., *Proc. 24th Int. Cosmic Ray Conf.* **1**, 758 (1995), Roma; R. Wischnewski, AMANDA Collaboration, *Nucl. Phys. B Proc. Suppl.* **110**, 510 (2002) (web page: <http://amanda.berkeley.edu/amanda/amanda.html>).
- [6] J. Ahrens et al., The IceCube Proposal to NSF (2000), J. Ahrens et al., PDD: IceCube Conceptual Design Document (2001); astro-ph/0209556 (web page: <http://icecube.wisc.edu>).
- [7] Antares Experiment Proposal, Antares Collaboration, astro-ph/9907432 and hep-ph/0211173 (web page: <http://antares.in2p3.fr>).
- [8] EUSO Collaboration, A. Petrolini for the collaboration, *Nucl. Phys. Proc. Suppl.* **113**, 329 (2002).

[9] for a study of the characteristics of charged primary air showers at large zenith angle, see M. Ave, R.A. Vázquez, and E. Zas, *Astropart. Phys.* **14**, 91 (2000); M. Ave, J.A. Hinton, R.A. Vázquez, A.A. Watson, and E. Zas, *Phys. Rev.* **D65**, 063007 (2002).

[10] G. Parente and E. Zas, *Proc. 7th Int. Work. on Neutrino Telescopes*, Venice (1996); P. Billoir, Auger Note **GAP-1997-049**; J.R. Jorwall, Auger Note **GAP-1997-074**; C.K. Guerard, Auger Note **GAP-2002-049**; Auger Note can be found at the address: http://www.auger.org/admin/GAP_Notes/index.html.

[11] X. Bertou, P. Billoir, and T. Pradier, Auger Note **GAP-1997-058**; S. Coutu, X. Bertou, and P. Billoir, Auger Note **GAP-1999-030**.

[12] D. Heck, J. Knapp, J.N. Capdevielle, G. Schatz, and T. Thouw, CORSIKA, **FZKA 6019** (1998), Forschungszentrum Karlsruhe (web page: <http://www-ik3.fzk.de/~heck/corsika>).

[13] S.J. Sciutto, astro-ph/9911331.

[14] G. Corcella, I.G. Knowles, G. Marchesini, S. Moretti, K. Odagiri, P. Richardson, M.H. Seymour, and B.R. Webber, HERWIG 6.5, *JHEP* **0101**, 010 (2001) [hep-ph/0011363]; hep-ph/0210213.

[15] K.-H. Kampert et al., Kascade collaboration, *Proc. 26th Int. Cosmic Ray Conf.* **3**, 159 (1999), Salt Lake City (USA); H.O. Klages et al., Kascade Collaboration, *Proc. 25th Int. Cosmic Ray Conf.* **6**, 141 (1997) and **8**, 297 (1997), Durban (South Africa).

[16] J.N. Capdevielle, *J. Phys. G: Nucl. Part. Phys.* **15**, 909 (1989).

[17] A. Capella and J. Tran Thanh Van, *Phys. Lett.* **B93**, 146 (1980); A. Capella et al., *Phys. Rep.* **236**, 225 (1994).

[18] K. Werner, *Phys. Rep.* **232**, 87 (1993).

[19] N.N. Kalmykov and S.S. Ostapchenko, *Yad. Fiz.* **56**, 105 (1993); *Phys At. Nucl.* **56** N3, 346 (1993); N.N. Kalmykov, S.S. Ostapchenko, and A.I. Pavlov, *Izv. RAN Ser. Fiz.* **58** N12, 21 (1994); N.N. Kalmykov, S.S. Ostapchenko, and A.I. Pavlov, *Bull.*

Russ. Acad. Science (Physics) **58**, 1966 (1994); N.N. Kalmykov, S.S. Ostapchenko, and A.I. Pavlov, *Nucl. Phys. B Proc. Suppl.* **52**, 17 (1997).

- [20] J. Ranft, *Phys. Rev.* **D51**, 64 (1995); hep-ph/9911213 and hep-ph/9911232.
- [21] T. Regge, *Nuovo Cimento* **14**, 951 (1959); V.N. Gribov, *Sov. Phys. JETP* **26**, 414 (1968).
- [22] R.S. Fletcher, T.K. Gaisser, P. Lipari, and T. Stanev, *Phys. Rev.* **D50**, 5710 (1994); J. Engel, T.K. Gaisser, P. Lipari, and T. Stanev, *Phys. Rev.* **D46**, 5013 (1992); R. Engel, T.K. Gaisser, P. Lipari, and T. Stanev, *Proc. 26th Int. Cosmic Ray Conf.* **1** (1999), Salt Lake City (USA).
- [23] H.J. Drescher, M. Hladik, S. Ostapchenko, T. Pierog, and K. Werner, *Phys. Rep.* **350**, 93 (2001).
- [24] H. Fesefeldt, Report **PITHA-85/02** (1985), RWTH Aachen.
- [25] S.A. Bass et al., *Prog. Part. Nucl. Phys.* **41**, 225 (1998); M. Bleicher et al., *J. Phys. G: Nucl. Part. Phys.* **25**, 1859 (1999).
- [26] L.D. Landau and I.Ya. Pomeranchuk, *Dokl. Akad. Nauk, SSSR* **92**, 535 and 735 (1953); A.B. Migdal, *Phys. Rev.* **103**, 1811 (1956).
- [27] A.A. Lagutin, A.V. Plyasheshnikov, and V.V Uchaikin, *Proc. 16th Int. Cosmic Ray Conf.* **7**, 18 (1979), Kyoto (Japan); J.N. Capdevielle for Kascade Collaboration, *Proc. 22nd Int. Cosmic Ray Conf.* **4**, 405 (1991), Dublin (Ireland).
- [28] S. Gieseke, *Proc. 14th Topical Conference on Hadron Collider Physics*, Karlsruhe, 2002 (web page: <http://www.hep.phy.cam.ac.uk/~gieseke/Herwig++/>).
- [29] A.D. Martin, R.G. Roberts, W.J. Stirling, and R.S. Thorne, *Phys. Lett.* **B443**, 301 (1998) [hep-ph/9808371].
- [30] CMZ (Code Management system using Zebra) User Guide and Reference Manual, CERN (1994) (web page: <http://wwwinfo.cern.ch/cmz>).

- [31] R. Gandhi, C. Quigg, M.H. Reno, and I. Sarcevic, *Phys. Rev.* **D58**, 093009 (1998).
- [32] the sample main can be found at the address:
<http://hepwww.rl.ac.uk/theory/seymour/herwig/herwig65.tst>.
- [33] F. Kakimoto, E.C. Loh, M. Nagano, H. Okuno, M. Teshima, and S. Ueno, *Nucl. Instr. Meth. A* **372**, 527 (1996); M. Risso and D. Heck, Auger Note, **GAP-2002-043**.